

On the response of Coastal Water to the intensification of East Korea Warm Current along the East Coast of Korea-A theoretical consideration

Young Ho Seung
Incheon 160 Korea

東韓暖流의 強化에 따른 沿岸水의 應答에 관한 理論的 高찰

承 永 鏞
인하대 해양학과

Abstract

The response of coastal waters to the summertime intensification of the East Korea Warm Current is considered theoretically. A simply analytic model explains well the development of southward coastal current in the north (37-38°N) and the uprising of lower cold water in the south (35-36°N). The mechanism involved is the Rossby adjustment to a sudden increase of current.

要約: 夏期 東韓暖流의 強化에 따른 沿岸水의 應答에 대하여 理論的으로 高찰하였다. 간단한 解析 모델을 이용하여 夏期 南向 沿岸流의 형성 (37°N 以北) 및 沿岸 底層冷水의 상승 (36°N 以南) 원인을 설명할 수 있었다. 이러한 현상의 미케니즘은 급격한 海流의 強化에 따른 로스비 變形 過程으로 밝혀졌다.

INTRODUCTION

Various coastal phenomena occurring along the east coast of Korea have long been one of the intense research subjects of many scientists. Among others, those by Lie (1984), Lie & Byun (1985), Lim and Chang (1969) and Lee & Na (1985) are quite interesting. The former two studies describe the summertime development of southward coastal current in the north (37-38°N), which is known as the North Korea Cold Current (hereafter NKCC). The persistent southward current in summer has already been remarked by KORDI (1981) in an analysis of current data observed also by KORDI (1980) in shallow coastal area.

The prominent feature of the observations

is that the isopycnals form a doming somewhat at about 50 Km from the coast. If we make further interpretations, this doming also indicates that northward current develops offshore on the other side of the dome as well as the development of southward current near the coast. In Lie & Byun's (1985) salinity section, the high salinity cores are seen at the offshore edge where the doming takes place. In fact, this edge (dome) may correspond to the boundary between the East Korea Warm Current (hereafter EKWC) offshore and the fresh coastal water inshore.

It has been generally known that the EKWC flows along the east coast of Korea and separates itself from the coast further north. The separation seems to take place near

36°N. The larger scale salinity sections based on the longterm (1961-1975) salinity measurements by Fisheries Research Development Agency (FRDA) show this nature as shown in Fig. 1 a, b and c for three representative sections. The high salinity water (EKWC water) touches the coast in the south (around 208 line) whereas lies offshore in the north (around 106 line). Lie & Byun's (1981) hydrographic observations cover in detail inshore

of the station 106-05 (about 50 Km from coast) which corresponds approximately to the offshore edge of their sections.

In the south (35-37°N), many observations reveal the summertime development of lower cold water near the coast. Lim and Chang (1969) first noted it in the Korea Strait. An (1974) remarked the same feature along the coast north of the Korea Strait. The lower cold water sometimes rises up to the surface making the coastal front there. It may also favor the wind-induced coastal upwelling (Seung, 1974; Lee and Na, 1985). Kim and Kim (1983) analyzed the water properties and drew a conclusion that the lower cold water in this area is an extension of the NKCC flowing southward along the coast. This current is believed to submerge as it flows southward by some mechanisms yet unknown. These studies indicate that the region considered here (35-36°N) corresponds to the southern limit of presence of the NKCC water.

In this paper, we therefore explain how these features can occur: development of southward coastal current (NKCC) in the north (37-38°N), and development of the lower cold water in the south (35-36°N). A simple analytic model is used to demonstrate the mechanism. The physical process involved is the Rossby adjustment to a sudden increase of current.

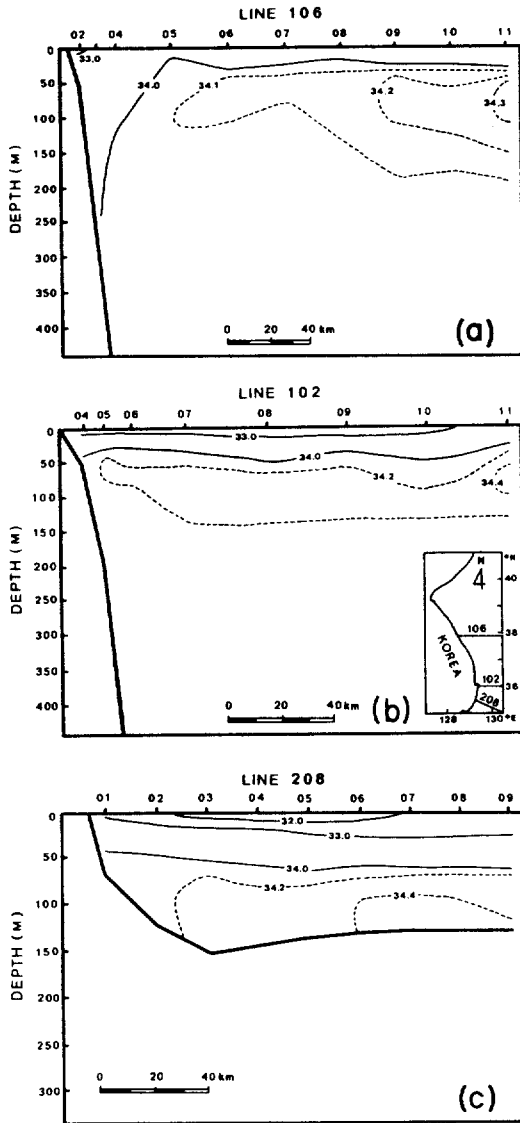


Fig. 1. Large scale salinity sections along the lines a) 106, b) 102 and c) 208 made by FRDA in August. Data are averaged over 1961-1975.

SOUTHWARD COASTAL CURRENT IN THE NORTH (37-38°N)

Consider a two-layer ocean initially at rest. The upper layer has the density ρ_1 and initial depth h_0 . The lower layer has the density ρ_2 and infinite depth. In the upper layer, the coastal water extends initially from $x = 0$ (coast) to $x = L$ farther offshore. Offshore of $x = L$, the EKWC water extends almost infinitely on the horizontal plane (Fig. 2).

This situation seems to correspond relatively well to the reality (c.f. Fig. 1a), at least for

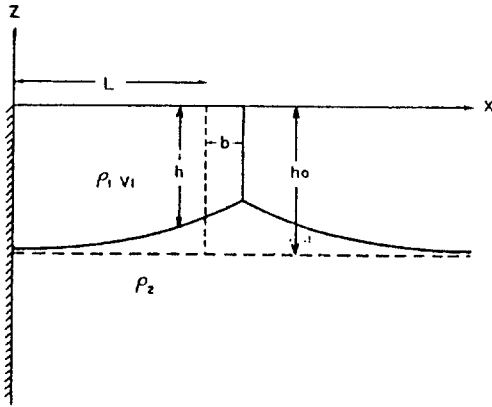


Fig. 2. Idealization of the study area, north (37-38°N) of the east coast. Dotted lines represent the initial state and solid lines denote the final state.

the modelling purpose. There is a discrepancy in assuming the homogeneous upper layer because, in real situation, density stratification persists due to the summer heating from above. This discrepancy does not matter much here as will be discussed later.

Through some mechanisms, a certain amount of momentum is given to the upper water columns extending over $x > L$ (EKWC water), i.e. it is suddenly endowed with a velocity v_0 in the y-direction (into the page). This sudden increase of velocity idealizes the summertime intensification of EKWC.

Without any balancing pressure gradient, the current thus moves to the right until enough of a pressure gradient checks further deflection. We express the final deflection by b (c.f. Fig. 2). Since the cross-stream movement (in the x-direction) is blocked by the presence of wall at the coast ($x=0$), horizontal divergence occurs near the coast. Consequently, the upper layer shrinks and the interface rises. However, the infinitely deep lower layer will remain motionless. The assumption of infinitely deep lower layer thus simplifies the problem while still allowing the response characteristics of the upper layer.

In presence of stratification in the upper

layer, this explanation will be valid more or less for each individual layer between two adjacent isopycnals. For initial momentum distributed uniformly over these individual layers, the integrated effect will then be nearly as same as that for the two layer ocean assumed here.

The current in the y-direction, v , is geostrophically balanced in the final state; conditions are assumed uniform in the y-direction. It is further assumed that the initial vorticity is conserved during the adjustment. Because there is no motion in the lower layer, the pressure gradient can be given only by the inclination of the interface and the surface elevation can be ignored. For inviscid fluid, the governing equations are then

$$fv = g' \partial h / \partial x \tag{1}$$

for geostrophic balance in the final state, and

$$(f + \zeta) / h = f / h_0 \tag{2}$$

for the conservation of potential vorticity. In the above equations, h denotes the upper layer depth; f is the Coriolis' parameter; $g' = g(\rho_2 - \rho_1) / \rho_2$ is the reduced gravity; and $\zeta = \partial v / \partial x$ is the relative vorticity. Meanwhile, the momentum equation in the y-direction is

$$dv / dt = -fu \tag{3}$$

at any time during the adjustment process.

The variables are non-dimensionalized as follows:

$$\begin{aligned} v &= fRv' \\ (x, b, L) &= R(x', b', L') \\ (h, h_0) &= h_0(h', 1) \end{aligned}$$

where the primes denote non-dimensionalization; $R = \sqrt{g'h} / f$ is the Rossby radius (b and L are already explained above). Hereafter, we drop the primes and all variables are assumed non-dimensionalized. Equations (1) and (2) then become

$$v = \partial h / \partial x \tag{1}'$$

$$\partial v / \partial x + 1 = h \tag{2}'$$

From Eqs (1)' and (2)', solutions for the final state are found as follows:

$$h = 1 + C_1 \cosh x + C_2 \sinh x \quad (4)$$

$$v = C_1 \sinh x + C_2 \cosh x \quad 0 < x < b + L \quad (5)$$

$$h = 1 + C_3 \text{Exp}(-x) \quad (6)$$

$$v = -C_3 \text{Exp}(-x) \quad b + L < x \quad (7)$$

The integral constants C_1 through C_3 and b are all yet to be determined. In obtaining solutions (6) and (7), the conditions of vanishing disturbances as $x \rightarrow \infty$ are imposed. Other conditions to be imposed are

$$v = 0 \quad \text{at} \quad x = 0 \quad (8)$$

$$v = -b \quad \text{at} \quad x = (L + b)^- \quad (9)$$

$$v = v_0 - b \quad \text{at} \quad x = (L + b)^+ \quad (10)$$

$$\int_0^{b+L} h dx = L \quad (11)$$

$$h[(L + b)^-] = h[(L + b)^+] \quad (12)$$

Equations (8) through (10) represent the fact that the increase in v of a given water column is determined by its total displacement in the x -direction (c.f. Eq. (3)). In Eqs (9) and (10), there is a velocity discontinuity at $x = L + b$. This is because the model is for inviscid fluid. Equation (11) expresses the mass conservation, which, when using Eq. (2)', becomes equivalent to Eqs (8) and (9). Equation (12) shows the continuity of h at $x = L + b$. Imposing these conditions to solutions (4) through (7) results in the following non-linear algebraic equations:

$$C_2 = 0 \quad (13)$$

$$C_1 \sinh(L + b) + b = 0 \quad (14)$$

$$C_3 \text{Exp}[-(L + b)] - b + v_0 = 0 \quad (15)$$

$$C_1 \cosh(L + b) - C_3 \text{Exp}[-(L + b)] = 0 \quad (16)$$

The four unknowns, C_1 through C_3 and b , can be determined by solving these non-linear equations numerically. Similar problems but for different cases are solved by Stommel and Veronis (1980), Van Heijst (1985) and Seung (1986).

However, analytic solutions can be obtained by assuming $L + b$ moderately larger than unity such that the hyperbolic functions in Eqs (14) and (16) can be approximated as $\text{Exp}(L + b)/2$: in real situation, $R \sim 10$ Km with $\rho_2 - \rho_1 \sim 1.0 \text{Kg/m}^3$, (dimensional) $h_0 \sim 100$ m and $f \sim 10^{-4} \text{sec}^{-1}$; b is the same order of magnitude as R ; and (dimensional) $L \sim 50$ Km. This approximation seems to be quite good and the resulting solutions are

$$h = 1 - v_0 \text{Exp}[-(v_0/2 + L)] \cosh x \quad (17)$$

$$v = -v_0 \text{Exp}[-(v_0/2 + L)] \sinh x \quad (18)$$

$$0 < x < b + L$$

$$h = 1 - (v_0/2) \text{Exp}(v_0/2 + L - x) \quad (19)$$

$$v = (v_0/2) \text{Exp}(v_0/2 + L - x) \quad (20)$$

$$b + L < x$$

with $b = v_0/2$. These solutions show that, near the boundary $x = b + L$, the offshore (EKWC) water loses half the initial velocity whereas the coastal water gains the same amount of speed in the opposite direction. The corresponding rise of interface at this point is proportional to the displacement of the boundary which, in turn, is proportional to the initial velocity. However, for an initial velocity v_0 (dimensional) = $2fR$, the interface touches the surface and the model begins to be no longer valid for larger v_0 . As an example, an initial velocity of 1 m/sec imposed offshore over 100m deep upper layer results in a coastal current of -0.5 m/sec inshore, with the interface rising up to 50 m at the final state.

DEVELOPMENT OF LOWER COASTAL WATER IN THE SOUTH (35-36°N)

Consider a two-layer ocean with finite depth in both layers. We use the same notations as before except that the upper layer and lower layer are represented by subscripts 1 and 2 respectively. The upper layer is filled by EKWC water with infinite horizontal extent

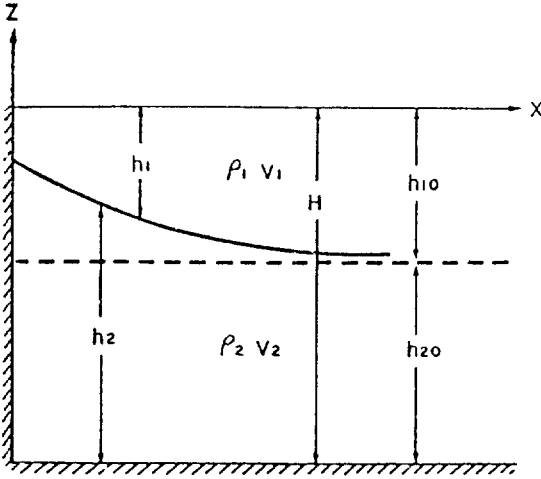


Fig. 3. As in Fig. 2 except for the south (35-36° N) of the east coast.

and the lower layer corresponds to the cold coastal water (Fig. 3).

Despite the limit of presence of the lower water in the south, we still assume that, near the northern limit of the region under consideration (near the line 102 in Fig. 1b), the alongshore variation can be neglected and the dynamics are locally the same as before. As for what goes on further south, discussions are made briefly at the end of this section.

We take the rigid lid surface. It has been demonstrated by Stommel & Veronis (1980) for a simple case of a surface-to-bottom front, that the interfacial shape remains virtually unchanged when the free surface is replaced by a rigid lid. All variables are non-dimensionalized in the same manner as before except for depth variables which are non-dimensionalized by the total depth H , i.e. $(h_1, h_2, h_{10}, h_{20}) = H (h_1', h_2', h_{10}', h_{20}')$ where h_{10} and h_{20} denote initial depths of the upper and lower layers respectively. Consequently, the Rossby radius is obtained by using this total depth, i.e. $R = \sqrt{g'H}/f$. The primes are dropped hereafter. The governing equations are then

$$v_1 - v_2 = \partial h_1 / \partial x \tag{21}$$

for the thermal wind relationship in the final state, and

$$\partial v_1 / \partial x + 1 = h_1 / h_{10} \tag{22}$$

$$\partial v_2 / \partial x + 1 = h_2 / h_{20} \tag{23}$$

for the conservation of potential vorticity. The total depth is remained constant, i.e.

$$h_1 + h_2 = 1 \tag{24}$$

From Eqs (21) through (24), the equation only for h_1 is obtained:

$$\partial^2 h_1 / \partial x^2 - (1/h_{10} + 1/h_{20}) h_1 = -1/h_{20} \tag{25}$$

Solving Eq. (25) and using Eqs (21) through (24) give the solutions for final state:

$$h_1 = h_{10} [1 + C_4 \text{Exp}(-\gamma x)] \tag{26}$$

$$v_1 = - (C_4 / \gamma) \text{Exp}(-\gamma x) + C_5 \tag{27}$$

$$h_2 = h_{20} - h_{10} C_4 \text{Exp}(-\gamma x) \tag{28}$$

$$v_2 = C_5 + (h_{10} C_4 \gamma - C_4 / \gamma) \text{Exp}(-\gamma x) \tag{29}$$

where $\gamma = (h_{10} h_{20})^{-1/2}$ is the inverse of disturbance scale; and C_4 and C_5 are integration constants yet to be determined. The condition of vanishing disturbances as $x \rightarrow \infty$ is already imposed. Other conditions are

$$v_1 = v_0 \quad \text{at} \quad x = 0 \tag{30}$$

$$v_2 = 0 \quad \text{at} \quad x = 0 \tag{31}$$

These conditions represent the fact that no momentum change occurs at the vertical wall because of no cross-stream displacement there (c.f. Eq. (3)). Application of Eqs (30) and (31) to Eqs (27) and (29) determines the unknowns, giving

$$h_1 = h_{10} [1 - v_0 \sqrt{h_{20}/h_{10}} \text{Exp}(-\gamma x)] \tag{32}$$

$$v_1 = v_0 [h_{10} + h_{20} \text{Exp}(-\gamma x)] \tag{33}$$

$$h_2 = h_{20} [1 + v_0 \sqrt{h_{10}/h_{20}} \text{Exp}(-\gamma x)] \tag{34}$$

$$v_2 = v_0 h_{10} [1 - \text{Exp}(-\gamma x)] \tag{35}$$

These solutions show that, at the coast, the interface rises proportionally with both the initial velocity v_0 and the scale of disturbance $\gamma = \sqrt{h_{10} h_{20}}$. Fig. 4 shows the dependence of interface elevation on v_0 and h_{10} . The rate of rise of interface with velocity is maximum when both layers have the same depths. For a lower layer much deeper than the upper layer, even a small initial velocity can raise the interface up to the surface. In the reverse case, the interface always remains far below the surface for any reasonable initial velocity.

Near the northern limit of the region under consideration, the lower layer seems to be deep enough (c.f. Fig. 1b) for the interface to be sensible to the velocity change. Further south, however, water depth decreases abruptly and the lower layer becomes much shallower (c.f. Fig. 1c); it may finally disappear somewhat near the southern limit of the region. In this case, the model does not predict any significant rise of interface. However, it can be expected that the (southward) propagating Kelvin waves, though not considered in this model, will later raise the in-

terface up to the same level as that near the northern limit. Associated with this, additional southward current will be induced in the lower layer.

CONCLUSION

A simple model studied in this paper describes relatively well the coastal water behavior observed along the east coast of Korea in summer, i.e. the development of NKCC in the north (37-36°N) and the lower cold water in the south (35-36°N). The mechanism involved is the Rossby adjustment to a sudden increase of EKWC in summer. A sudden increase of current without any balancing pressure gradient adjusts itself to the geostrophic equilibrium by building up the appropriate pressure gradient. In this process, water columns deflect to the right of current direction thus raising the interface and creating the additional momentum.

This model does not provide any connection between the north and south regions, which necessarily involves the longshore variation. Future studies may then have to be focused on this point. Finally, it should be mentioned that the EKWC system varies from year to year so that there may be some occasions where the model cannot be applied.

ACKNOWLEDGEMENTS

The author thanks to drs H.J. Lie, S.K. Byun and other colleagues in the Physical Oceanography Laboratory of KORDI for discussions. He also thanks to Mr. P.H. Lee and C.H. Cho for drawings and typings. Comments from unknown referees are acknowledged too.

REFERENCES

- An, H.S., 1974. On the cold water mass around the southeast coast of Korean Peninsula. *J. Oceanol. Soc. Korea*, 9: 10-18.

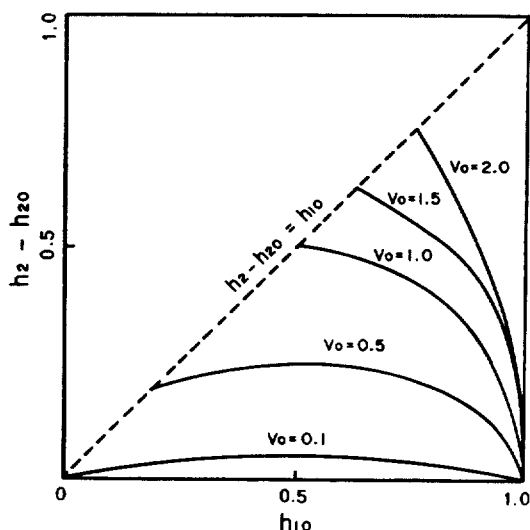


Fig. 4. Displacement of the interface as a function of initial upper layer depth h_{10} and initial velocity v_0 . Depths normalized by the total depth, H , and velocity by fR ; f is Coriolis' parameter and $R = \sqrt{g'H}/f$ is the Rossby radius. The dotted line denotes the surfacing of interface.

- Kim, C.H. and K. Kim, 1983. Characteristics and origin of the cold water mass along the east coast of Korea. *J. Oceanol. Soc. Korea*, **18**: 73-83. (in Korean)
- KORDI, 1980. Oceanographic studies for Ulijin Nuclear Power Plant. KORDI Rep. BSP100022-39-1, 277pp.
- KORDI, 1981. Dynamics of the costal water along the east coast of Korea. KORDI Rep. BSP100036-54-1, 62pp. (in Korean)
- Lee, J.C. and J.Y. Na, 1985. Structure of upwelling off the southeast coast of Korea. *J. Oceanol. Soc. Korea*, **20**: 6-19.
- Lie, H.J., 1984. Coastal current and its variation along the east coast of Korea. In *Ocean Hydrodynamics of The Japan and East China Seas*. Ed. T. Ichiye, 399-408, Elsevier Sci. Pub. Amsterdam.
- Lie, H.J. and S.K. Byun, 1985. Summertime southward current along the east coast of Korea. *J. Oceanol. Soc. Korea*, **20**: 22-27.
- Lim, D.B. and S.D. Chang, 1969. On the cold water mass in the Korea Strait. *J. Oceanol. Soc. Korea*, **4**: 71-82.
- Seung, Y.H., 1974. A dynamic consideration on the temperature distribution in the east coast of Korea in August. *J. Oceanol. Soc. Korea*, **9**: 52-28. (in Korean)
- Seung, Y.H., 1986. A bouyancy driven cyclonic gyre in the Labrador Sea. Accepted by *J. Phys. Oceanogr.*
- Stommel, H. and G. Veronis, 1980. Barotropic response to cooling. *J. Geophys. Res.*, **85**: 6661-6666.
- Van Heijst, G.J.F., 1985. A geostrophic adjustment model of a tidal mixing front. *J. Phys. Oceanogr.*, **14**: 1182-1190.

Received October 27, 1986

Accepted November 18, 1986